Werk

Jahr: 1983
Kollektion: fid.geo
Signatur: 8 Z NAT 2148:52
Digitalisiert: Niedersächsische Staats- und Universitätsbibliothek Göttingen
Werk Id: PPN1015067948_0052
PURL: http://resolver.sub.uni-goettingen.de/purl?PPN1015067948_0052

LOG Id: LOG_0047
LOG Titel: Energy and charge distribution of engergetic helium ions in the outer radiation belt of the earth
LOG Typ: article

Übergeordnetes Werk

Werk Id: PPN1015067948
PURL: http://resolver.sub.uni-goettingen.de/purl?PPN1015067948
OPAC: http://opac.sub.uni-goettingen.de/DB=1/PPN?PPN=1015067948

Contact

Niedersächsische Staats- und Universitätsbibliothek Göttingen
Georg-August-Universität Göttingen
Platz der Göttinger Sieben 1
37073 Göttingen
Germany
Email: gdz@sub.uni-goettingen.de

J Geophys (1983) 52:239–246

Journal of Geophysics

Energy and Charge Distribution of Energetic Helium Ions in the Outer Radiation Belt of the Earth*

B. Klecker[1], D. Hovestadt[1], M. Scholer[1], G. Gloeckler[2], F.M. Ipavich[2], and C.Y. Fan[3]

[1] Max-Planck-Institut für Physik und Astrophysik, Institut für extraterrestrische Physik, D-8046 Garching, Federal Republic of Germany
[2] University of Maryland, Department of Physics and Astronomy, College Park, MD 20742, USA
[3] University of Arizona, Department of Physics, Tucson, AZ 85721, USA

Abstract. We report the first direct determination of the charge states of energetic helium ions in the outer radiation belt. Our measurements, in the range $L=3$–4, revealed unexpected high fluxes of singly ionized helium below 1 MeV/nucleon: We found a He^+/He^{2+} ratio of 0.4 ± 0.1 at $L=3.3$ with a steep decrease to ~0.04 at $L=3.7$ at energies of 0.50–0.57 MeV/nucleon. The data were obtained with the MPE/UoMd experiment aboard the ISEE-1 spacecraft during a near equator ($B/B_0<1.025$) perigee pass on 17 Nov 1977. The observations suggest that fast cross-L transport during magnetic storms and non-adiabatic motion may play an important role for the distribution of helium ions at MeV energies in the outer radiation belt.

Key words: Earth's outer radiation belt – Helium ionic charge composition – Radial diffusion

Introduction

The observation of ions heavier than protons in the Earth's radiation belt has been recognized for a long time as providing a test for our understanding of radiation belt acceleration, propagation and loss processes (Cornwall, 1972; Krimigis, 1973; Blake, 1973). In addition, these tracer ions give unique insight into the sources of the trapped radiation: Large He^+ and O^+ fluxes at suprathermal energies as discovered at low altitudes and in the storm-time ring current (Shelley et al., 1972; Sharp et al., 1974, 1977; Balsiger et al., 1980) suggest strongly that the ionosphere is an important source of the trapped radiation. At somewhat higher energies ($\gtrsim0.4$ MeV/nucleon) the first unambiguous measurement of carbon and oxygen ions reported by Hovestadt et al. (1978a) revealed a C/O-ratio of ~1 at $L>2.7$, thus given strong support for the idea of an extraterrestrial source of these more energetic trapped ions in the outer radiation belt. Furthermore, there is now increasing evidence that heavy ions are not always a minor species but may also in part determine the radiation belt dynamics: Tinsley (1976) and Lyons and Evans (1976), for example, pointed out that at ring-current energies $Z>1$ ions (possibly He^+) rather than protons may be the dominant species.

Observations on the distribution of energetic helium in the Earth's radiation belt have been reported by many authors (Blake and Paulikas, 1972; Fritz and Williams, 1973; Fennell et al., 1974; and more recently by Fritz and Spjeldvik, 1978; Hovestadt et al., 1978a, 1981a; Blake et al., 1980; Spjeldvik and Fritz, 1981). These observational results have been complemented by extensive numerical calculations, modeling the transport of energetic ions in the radiation belt (Cornwall, 1972; Spjeldvik and Fritz, 1978a, b). These computations demonstrated the fundamental importance of charge exchange reactions for the distribution of heavy ions in the stationary radiation belt.

The model calculations predict, that, at low energies (<0.25 MeV/nuc) and small L-values ($L\lesssim3$), singly ionized helium is more abundant than doubly ionized helium. At higher energies (>0.5 MeV/nuc), however, doubly ionized helium dominates over He^+. These results are derived for a quiet magnetosphere assuming steady state conditions. If nonstationary transport during geomagnetically disturbed time periods plays a significant role, deviations from the stationary charge state distributions can be expected. A direct measurement of the ion charge states in the MeV energy range was, until recently, beyond experimental capabilities. In this paper we report the first direct measurement of the charge states of helium at energies >0.5 MeV/nucleon obtained with the Max-Planck-Institut/University of Maryland experiment aboard the ISEE-1 spacecraft in 1977.

Satellite and Instrumentation

The data were obtained with the Ultra-Low-Energy-Z-E-Q measuring analyzer (ULEZEQ) of the Max-Planck-Institut/University of Maryland experiment on ISEE-1.

The ISEE-1 satellite was launched into an eccentric orbit with an initial apogee of ~23 R_E, a perigee of ~600 km, an inclination of 28.7° and a period of ~57 h. During the first months of the mission the spacecraft moved, during one out of five low altitude passes, close to the geomagnetic equator over an extended range of L-values. Thus it is possible to study the characteristics of equatorially mirroring ions in great detail.

The ULEZEQ sensor is mounted with its look direction perpendicular to the spin axis of ISEE-1, which is spinning nearly perpendicular to the ecliptic plane at ~20 rpm. The sensor combines the energy/charge determination in an electrostatic deflection analyzer with a dE/dx vs E measurement

* Based on a paper given at the Symposium on Plasma and Energetic Particles in the Magnetosphere, EGS Meeting, 23–27 August 1982, Leeds, U.K.

Offprint requests to: B. Klecker

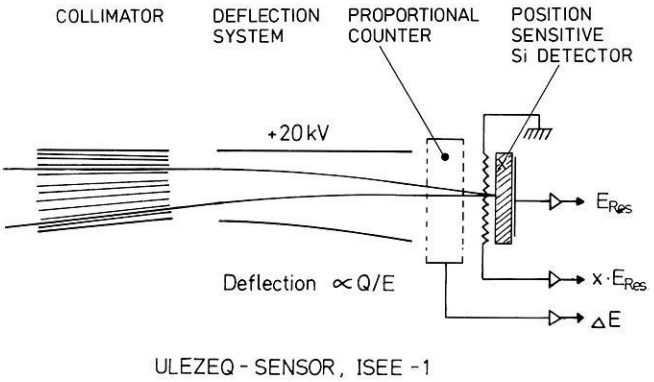

Fig. 1. Cross-sectional view of the ULEZEQ sensor on ISEE-1

Table 1. ULEZEQ Response[a]

Rate-ID	Particle	Energy range	Comment
UHP 1	proton	0.45–1.2 MeV/nuc	Rate channel
UHP 2	proton	1.20–3.0 MeV/nuc	Rate channel
UHA	helium	0.25–3.0 MeV/nuc	Rate channel
UHH	$Z>2$	>0.3 MeV/nuc (O)	Rate channel
		>0.2 MeV/nuc (Fe)	Rate channel
HE 1	helium	0.42–0.50 MeV/nuc	PHA events,
HE 2	helium	0.50–0.57 MeV/nuc	normalized with
HE 3	helium	0.57–0.67 MeV/nuc	UHA-rate.
HE 4	helium	0.67–0.95 MeV/nuc	

[a] Geometrical Factor: $\sim 0.02\ cm^2 sr$

to derive both the ionic and nuclear charge as well as the energy of the particles between 0.3 and 3 MeV/nucleon. A schematic cross section of the sensor is shown in Fig. 1. For ions passing through the multislit collimator and the electrostatic deflection analyzer and stopping in the position sensitive solid state detector (PSD), three parameters are measured: (1) the energy loss, ΔE, in a thin window, flow-through, proportional counter (PC), (2) the deflection, x, and (3) the residual energy, E_{Res}, in the position sensitive detector. These three parameters, in principle, unambiguously determine the nuclear charge Z, the ionic charge Q, and the energy E of the incoming ion. The energy response of the sensor is summarized in Table 1. A detailed description of the experiment may be found elsewhere (Hovestadt et al., 1978b).

Charge Determination

The ionic charge Q can be derived from the position signal (x. E_{Res}) and the incident energy (E_{in}) of the particles. However, due to non-uniformities in the resistive layer (palladium) of the position sensitive detector, which were established after the launch of ISEE-1, the position signal does not depend linearly on the actual deflection of the particles. In order to regain the position calibration we evaluated the position response of the PSD of our experiment on ISEE-1 using in-flight data obtained during a large solar flare in September 1978. Figure 2 shows the position response for He^{2+} as a function of incident energy. The corresponding response of the PSD of our sensor of identical design on ISEE-3 is shown for comparison. The unit of the position response corresponds to the maximum deflection of the ions. Figure 2 indicates that the position signal

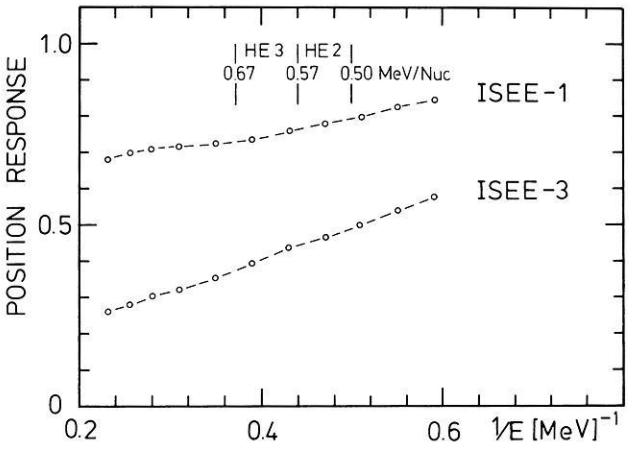

Fig. 2. Position response of the position sensitive detectors on ISEE-1 and ISEE-3, respectively. Data obtained for a large solar flare (day 268 0:00–270 11.00 UT, 1978) have been used

of the PSD on ISEE-1 becomes insensitive to the actual deflection at energies $\gtrsim 0.7$ MeV/nucleon. We restricted the charge analysis therefore to the energy range 0.5–0.67 MeV/nucleon, where the charge resolution, although degraded relative to ISEE-3, is sufficient to separate clearly the helium charge states. This energy range has been subdivided into two energy bins, denoted HE 2 and HE 3, in Fig. 2.

Observations

We analyzed the helium charge state distribution during the low altitude pass of ISEE-1 on 17 Nov 1977. This orbit was selected because the magnetosphere was reasonably quiet during this day ($Kp<3$, $DST>-50\ \gamma$) and the time period met our requirements of (1) having good data coverage and high time resolution due to high data rate and (2) ISEE-1 being close to the geomagnetic equator. It should, however, be noted that the preceding period of 6 days was not quiet with an average Kp index of ~ 4 and a maximum Kp value of 6^- for 6 h. During the time period analyzed, ISEE-1 was very close to the equator ($B/B_0<1.025$). This is essential for the present analysis: Due to the pitch angle distribution of equatorially mirroring helium ions, which is sharply peaked at 90° (Fritz and Williams, 1973; Blake et al., 1980; Hovestadt et al., 1981a; Fritz and Spjeldvik, 1982), the counting statistic for off-equator passes would not be sufficient for a detailed charge analysis with good spatial resolution.

We restricted our analysis to $L>3.2$ in order to minimize the influence of the background due to the high fluxes of energetic protons. Figure 3 shows a typical example of the ΔE versus E_{Res} pulse height matrix obtained during the time period 20:46–20:51 UT on 17 Nov 1977, ($L=3.6$–3.8). HE 1, HE 2, HE 3, and HE 4 denote four boxes along the He-track used for the evaluation of helium energy spectra. The energy scale indicates the incident energy of ^{4}He ions. This pulse height matrix demonstrates that protons, pile-up counts produced by protons, and helium ions are clearly separated. Note that the number of events along the proton track is considerably reduced relative to the helium and proton pile-up counts. This is due to the electronic selection system which significantly suppresses all counts in the shaded lower left area of the matrix.

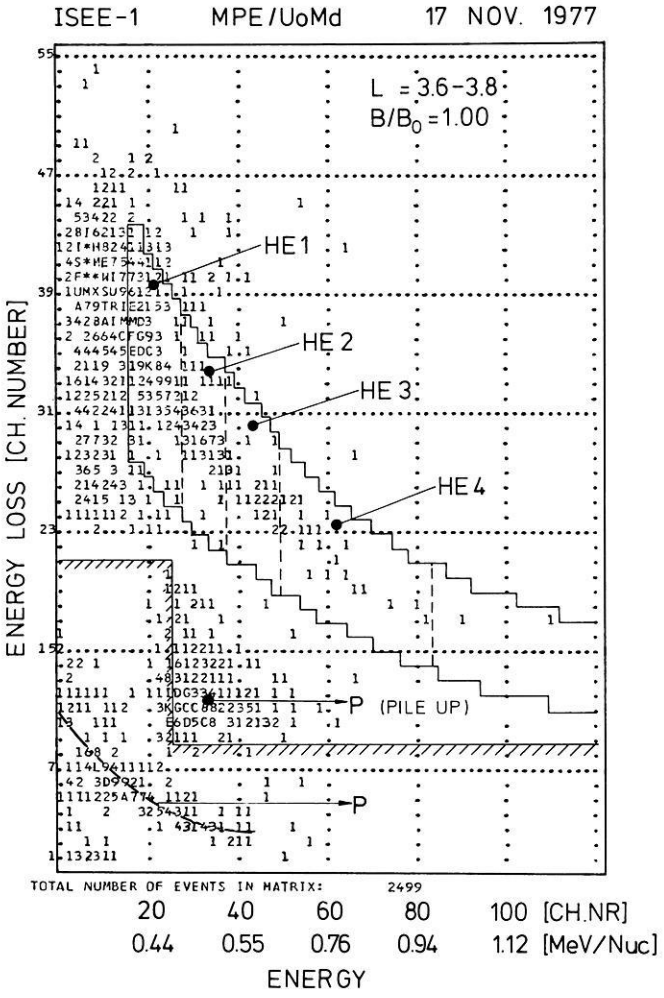

Fig. 3. Energy loss versus residual energy pulse-height matrix accumulated during the near equator perigee pass of ISEE-1 on 17 Nov 1977, (20:46–20:51 UT)

Helium Charge Analysis

Ionic charge histograms for helium ions are derived by first preselecting the helium in the ΔE versus E_{Res} pulse height matrix and subsequently converting the position signal into a charge scale using the results of the ISEE-1 in-flight calibration as described above. In Fig. 4 helium charge histograms are presented for two energy ranges (0.5–0.57, 0.57–0.67 MeV/Nuc, labelled HE 2 and HE 3 in Fig. 3) and for four L-intervals between $L=3.2$ and $L=4.0$. We find a significant amount of singly ionized helium at low L-values ($L \lesssim 3.6$) in both energy ranges with a drop of the He^+/He^{2+}-ratio down to the sensitivity level of the experiment at $L \gtrsim 3.6$. The maxima of the charge histograms in the higher energy range (right panel) are not centered at integral charge state numbers. This reflects the uncertainties in the charge determination of helium which become larger with increasing energy. The L-dependence of the He^+/He^{2+}-ratio in the energy range 0.50–0.57 MeV/nucleon is shown more quantitatively in Fig. 5. The He^+/He^{2+}-ratios have been derived by fitting two gaussians to the corresponding charge histograms H(Q) of Fig. 4, using a least square fit procedure with 5 free parameters:

$$F(Q)=\alpha_0+\alpha_1\exp\left[-\left(\frac{Q-0.5Q_2}{\Delta Q}\right)^2\right]+\alpha_2\exp\left[-\left(\frac{Q-Q_2}{\Delta Q}\right)^2\right]. \quad (1)$$

$F(Q)$ is optimized with respect to the coefficients α_1, α_2, and a possible background α_0 using a linear regression procedure. The width of the charge distribution (characterized by ΔQ) and the center of the He^{2+} distribution (Q_2) are adjusted by an iterative method to allow for small variations in the instrumental parameters.

The resulting minimum variance double gaussian $F(Q)$ is shown in Fig. 4 (dashed lines). The He^+/He^{2+}-ratios are calculated by numerically integrating the gaussian fits to the distributions of He^+ and He^{2+}. The errors as given in Fig. 5 are derived as a combination of the standard deviation of the fit and the statistical errors resulting from the integrals of the He^+ and He^{2+} distribution, respectively. It can be seen in Fig. 5 that the He^+/He^{2+}-ratio drops from 0.4 ± 0.1 at $L=3.2$–3.4 to 0.075 ± 0.03 at $L=3.4$–3.6 and to ~ 0.04 at $L>3.6$.

Energy Spectra and Distribution Function

Perpendicular differential helium fluxes ($j_\perp$) at the equator ($B/B_0<1.025$) are presented in Fig. 6. These fluxes have been derived from spin averages of the helium pulse height matrices and of the total helium counting rate, using the given angle between the spacecraft spin axis and the local magnetic field direction. For the pitch-angle distribution of helium ions the functional form $j(\alpha)=j_\perp\cdot\sin^n(\alpha)=j_\perp\cdot(B/B_0)^{n/2}$ has been assumed, where α is the pitch angle of the particles. For n a value of 10 has been used which is in good agreement with experimental results in this energy range (Blake et al., 1980; Hovestadt et al., 1981a; Fritz and Spjeldvik, 1982). The helium pulse height counts are converted to $j_\perp$ on a 64 s time basis. Figure 6 shows that the helium spectra steepen considerably with increasing L-value with a spectral index $\gamma=-4.3$ at $L=3.5$ and $\gamma=-7.1$ at $L=3.9$. With the spectra of equatorially mirroring helium ions as a function of L-value we are able to calculate the distribution function $f\sim j_\perp\cdot L^3$ for several values of the first adiabatic invariant μ. Figure 7 shows the distribution function of helium for several values of the magnetic moment μ (200–600 MeV/Gauss). Above $L\sim 3.5$ these curves have a positive slope indicating an inward radial transport of these ions. It should be noted that this result is derived for the total ($He^+ + He^{2+}$) helium population. The individual distribution functions of He^+ and He^{2+} cannot be calculated because the ionic charge analysis is only possible for a very limited energy range, as discussed above.

Discussion

The results of our analysis of the energy spectra and ionic charge composition of helium during the near equator perigee pass of ISEE-1 on 17 Nov 1977, can be summarized as follows:

– significant fluxes of singly ionized helium ($HE^+/He^{2+}=0.4\pm0.1$) have been observed at low L-values ($L=3.3$)

– the He^+/He^{2+}-ratio exhibits a sudden decrease from a value of ~ 0.4 at $L=3.3$ to ~ 0.04 at $L=3.7$

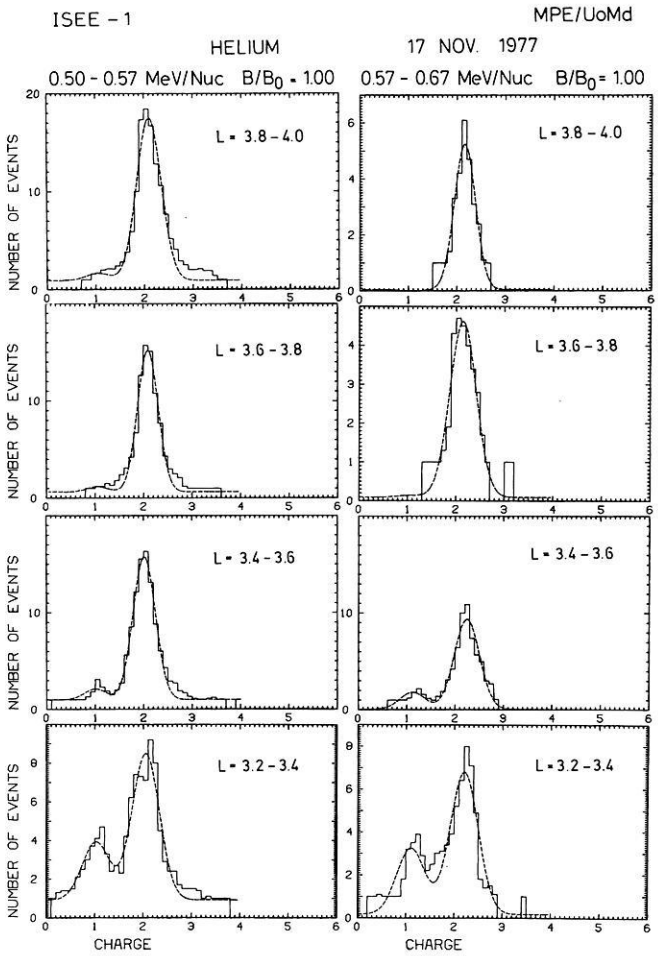

Fig. 4. Helium charge histograms in the energy range 0.50–0.67 MeV/nuc obtained on ISEE-1 during the near equator perigee pass on 17 Nov 1977

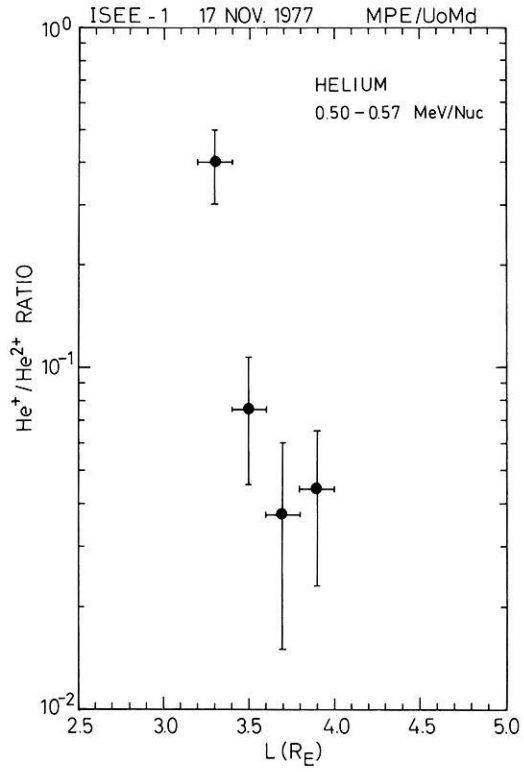

Fig. 5. He^+/He^{2+}-ratio in the energy range 0.50–0.57 MeV/nuc as a function of L-value. The ratios are derived from the double-gaussian fit shown in Fig. 4 (*left panels*)

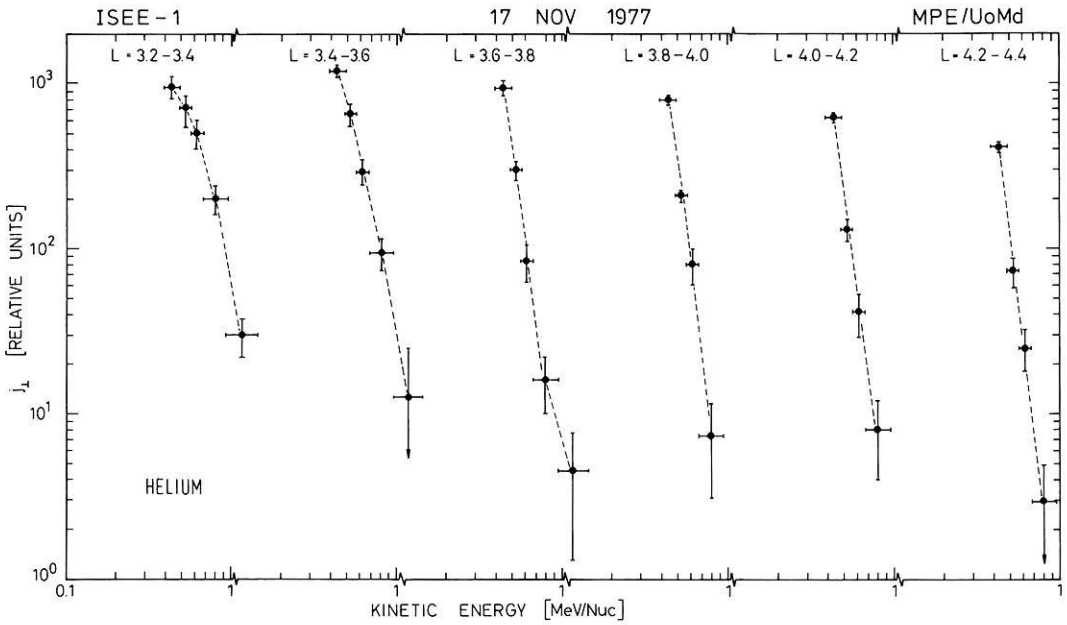

Fig. 6. Helium energy spectra in the L-range 3.2–4.4 as obtained on ISEE-1 during a near equator perigee pass ($B/B_0 < 1.025$) on 17 Nov 1977

– the helium energy spectra at the equator become steeper with increasing distance from the Earth

– the distribution function $f(\mu, L)$ of helium, evaluated at constant magnetic moment (200–600 MeV/Gauss) exhibits a positive radial gradient for $L \gtrsim 3.5$.

Among these results the most striking feature is the high He^+/He^{2+}-ratio at $L=3.3$ and the steep decrease towards higher L-values. The positive slope of the helium distribution function $f(L)$ and the steepening of the spectra with increasing distance from the Earth are, at least qualitatively, consistent with conventional steady state radial diffusion models, where the particle distribution is determined by cross-L diffusion from an outer boundary to the inner radiation belt and by losses due to charge exchange reactions and coulomb interactions. However, the sudden decrease of the He^+/He^{2+}-ratio as observed between $L=3.3$ and 3.7 during the perigee pass on 17 Nov 1977, seems to be not consistent with such a stationary model.

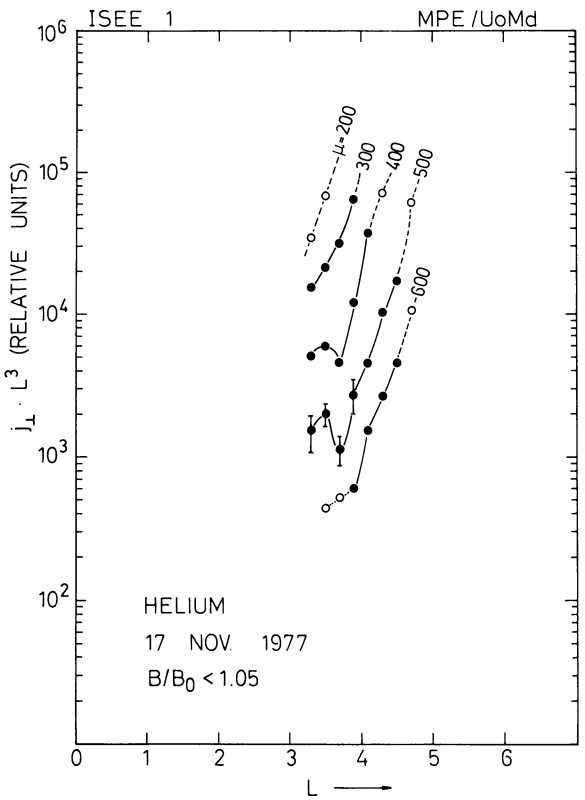

Fig. 7. Distribution function of helium derived at constant magnetic moment. Open circles indicate that extrapolations of the energy spectra as shown in Fig. 6 have been used

The numerical calculations of Spjeldvik and Fritz (1978a, 1981) showed that, for steady state conditions, the He^+/He^{2+}-ratio at 0.5 MeV/nucleon is almost constant with L. Spjeldvik and Fritz (1981) obtained $He^+/He^{2+} \sim 0.02$–0.03 between $L=3$ and 5. Cornwall (1972) also obtained $He^+/He^{2+} \sim$ const with L but with a much higher value of ~ 0.5–1.0 between $L=3$ and 4.5 at 0.5 MeV/nucleon. However, this discrepancy may be due to the different boundary conditions in μ-space and/or to different values of the charge exchange cross sections used by Cornwall (1972). Furthermore, the upper boundary in μ-space was, in his calculation, at $\mu=880$ MeV/Gauss and thus may strongly influence the results at 0.5 MeV/nucleon, which corresponds to $\mu > 230$ MeV/Gauss for $L > 3.3$.

Both model calculations revealed small variations of the He^+/He^{2+}-ratio with L which are certainly much less than the factor of ~ 10 observed during the perigee pass on 17 Nov 1977. Qualitatively, only a small variation of the He^+/He^{2+}-ratio with radial distance (at constant energy) can be expected, because in this range of energies and L-values the He^+/He^{2+}-ratio is determined predominantly by charge exchange reactions. This is due to the fact that at $L \sim 3$–4 and $E \sim 0.5$ MeV/nucleon, the typical time scales for coulomb energy degradation, charge exchange losses, and diffusive transport during magnetospherically quiet times are much larger than the time scales for charge exchange reactions. This is illustrated in Table 2 which shows typical transport and loss time scales for energetic helium ions in the radiation belt. The time scales for coulomb losses (τ_{Cb}) and charge exchange losses (τ_{CE}) are taken from Spjeldvik and Fritz (1981). The time scale for diffusive transport (τ_D) has been calculated adopting

$$D_{LL} = 2 \times 10^{-10} \cdot L^{10} + 2 \times 10^{-5} \cdot L^{10} / (L^4 + (\mu/Q)^2)\ [R_e^2/d] \quad (2)$$

for the radial diffusion coefficient, where the first term is due to magnetic field fluctuations and the second term arises from electric field fluctuations; μ and Q are the magnetic moment in MeV/Gauss and the ionic charge, respectively. The same function D_{LL} has been used by Spjeldvik (1977) and by Spjeldvik and Fritz (1978a) for their model calculations of proton and helium ion distributions in the quiet time radiation belt and resulted in a reasonably good fit to their quiet time experimental data. The time scales for charge exchange reactions $\tau_{12}(He^+ \rightarrow He^{2+})$ and $\tau_{21}(He^{2+} \rightarrow He^+)$ have been calculated with

$$\tau_{ij} = [\sigma_{ij} \langle H \rangle v]^{-1} \quad (3)$$

Table 2. Typical transport and loss time scales for energetic helium ions in the radiation belt

L	E	τ_{Cb} [a]	τ_{CE} [a]	τ_D [b]		τ_{21}	τ_{12}
				He^+	He^{2+}		
	(MeV/nuc)	(days)	(days)	(days)		(days)	(days)
2.95	0.5	412	54,500	21,400	6,420	151	2.2
3.55	0.5	965	71,400	7,100	2,700	290	4.2
4.0	0.5	1,660	115,000	2,990	1,420	433	6.3
4.45	0.5	19,000	174,000	1,250	730	590	8.6
5.05	0.5	308,000	240,000	404	292	900	14.5

[a] Spjeldvik and Fritz, 1981
[b] Calculated with Eq. (2)

using the charge exchange cross sections (σ_{ij}) given in Spjeldvik and Fritz (1978a) and assuming a neutral hydrogen density ($\langle H \rangle$) of the Earth's exosphere (at a temperature of 950° K) as given by Tinsley (1976). The time scales derived with (3) will, of course, rely strongly on the accuracy of the charge exchange cross sections used. The cross sections compiled by Spjeldvik and Fritz (1978a), however, seem to agree reasonably well with experimental values (Allison, 1958; Pivovar et al., 1962).

From Table 2 it can be seen that the dominant (smallest) time scales, determining the relative abundance of He^+ and He^{2+}, are τ_{12} and τ_{21} and that the dominant loss process for He^+ in this range of energy and radial distance is the $He^+ \rightarrow He^{2+}$ charge exchange reaction with a time scale τ_{12} of only ~ 6 days at $L=4$. Because of this small time scale it is unlikely that small variations of the parameters used for the model calculations may result in drastic changes of the radial dependence of the He^+/He^{2+}-ratio. However, non-stationary processes on time scales $\tau \sim \tau_{12}$ could result in large deviations from the stationary distribution of helium ions.

Non-Stationary Processes

The perigee pass on 17 Nov 1977 is in the recovery phase of a magnetic storm ($DST \sim -75$ nT) with increased geomagnetic activity (maximum $Kp \sim 6^-$) starting about 6 days before our measurement. Therefore, it is conceivable that non-stationary processes such as direct injection of helium ions into the region $L \sim 3.2$–3.6 or fast (adiabatic) cross-L transport may be important. The latter has been proposed, for example by Lyons and Williams (1980), to explain sudden temporal changes of the trapped proton distribution in the outer radiation belt. Below we will discuss both possibilities briefly.

(1) Direct Injection of Energetic Solar Helium Ions. Although the possibility of direct trapping of solar particles has been discarded until recently (Krimigis, 1970; Blake and Paulikas, 1972), the study of helium ions during magnetic storms by Spjeldvik and Fritz (1981) appears to suggest that non-diffusive injection processes occasionally play an important role during geomagnetic disturbances following large solar particle events. Furthermore, large abundances of singly ionized helium in low energy solar flare particles ($He^+/He^{2+} \sim .20$) have been discovered recently (Hovestadt et al., 1981b). However, neither shortly before nor after the perigee pass under discussion has an intensity increase of the low energy solar ion population been observed in interplanetary space. Therefore, we conclude that direct injection of solar particles is not very likely to constitute the source of He^+ observed on 17 Nov 1977, although it may be important for the 4 Aug 1972 event studied by Spjeldvik and Fritz (1981).

(2) Fast Cross-L Drift of the Ions: Lyons and Williams (1980) explained flux increases in the trapped low energy ion population observed during geomagnetic storms at $L=$ 2.5–4 by an inward drift of the ions, driven by an equatorial azimuthal electric field. The time scale of this process is of the order of the drift period and would be sufficiently fast to transport singly ionized helium down to $L=3.3$. However, Lyons and Williams (1980) did not observe an inward drift at energies $\gtrsim 100$ keV. The latter fact is a natural consequence of the proposed drift mechanism which is effective only for ions with a drift period comparable to or larger then the time scale for which large azimuthal electric fields exist (typical a few hours, the time scale of a magnetic storm). The drift period of equatorically mirroring non-relativistic ions in a dipole field is given by

$$\tau_{drift} = 0.73 \cdot \frac{Q}{E} \cdot \frac{1}{L} \text{ hours}, \tag{4}$$

where E is the energy of the ions in MeV. Thus, the drift period at 2 MeV for singly ionized helium at $L=3.5$ is only 6 min and a factor of 20 smaller than the drift period of 100 keV protons. Therefore it seems unlikely that this process could lead to effective radial transport in the energy range of our observations.

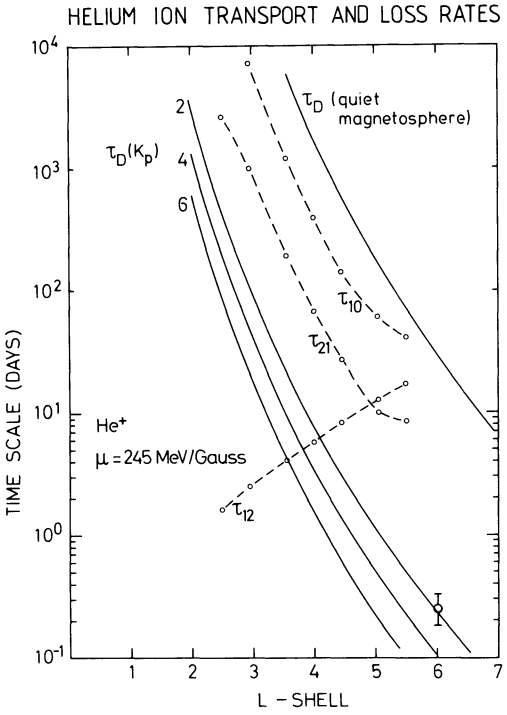

Fig. 8. Typical time scales for helium charge exchange reactions (*circles, interpolated by dashed lines*) and diffusive radial transport during magnetospherically quiet times and disturbed time periods (*heavy lines*). All time scales have been calculated for helium ions with $\mu = 245$ MeV/Gauss, the diffusion time scales have been calculated for He^+

(3) Fast Diffusive Transport. Another possibility is a fast diffusive transport of the helium ions. During the 4 days of increased geomagnetic activity preceding our measurement the Kp index was ~ 5 for a 24 h time period with a maximum value of 6^- for 6 h. It is conceivable that the radial diffusion coefficient was greatly increased and, consequently, the time scale for radial diffusion was significantly reduced during this time period, as illustrated in Fig. 8. The three curves labelled $Kp=2$, 4, 6 show the time scale for radial diffusion assuming nonstationary radial transport ($\mu=$ const) by azimuthal electric field fluctuations. For the equatorial power spectra $P(\nu)$ of electric field fluctuations an empirical formula of Mozer (1971) has been used which takes into account the Kp-dependence of $P(\nu)$:

$$P_i(\nu) = 100^{+200}_{-70} \exp(0.4\, Kp)\, \nu^{-1.6 \pm 0.3}\ (\text{mV})^2/\text{m}^2\text{Hz} \tag{5}$$

$P_i(v)$ is the power in the ith component of the perpendicular (azimuthal and radial) electric field fluctuations at the equator and v the particle drift frequency in cph. The relation between the electric field power spectrum and the diffusion time scale is given by (Fälthammar, 1965):

$$\tau_D \sim \frac{4B_0^2}{P(v)}. \quad (6)$$

Taking the first Fourier component and the maximum value in the allowed parameter range of (5), we calculated the minimum value of τ_D for singly ionized helium at 245 MeV/Gauss. The data point at $L=6$ has been calculated from another measurement of electric field power spectra by Holzworth and Mozer (1979) during a time period with an average Kp index of ~ 2. The typical time scale τ_D obtained with (2) for a quiet magnetosphere is shown for comparison. Also shown in Fig. 8 are the time scales τ_{10}, τ_{12}, and τ_{21} for charge exchange reactions, evaluated with (3) at constant magnetic moment $\mu = 245$ MeV/Gauss, which corresponds to $E = 0.53$ MeV/nucleon at $L = 3.3$. It is evident from Fig. 8 that fast cross-L diffusion of low energy helium ions during magnetospherically disturbed time periods on time scales comparable with the charge exchange time scale τ_{12} seems to be possible. At low energies and large radial distances, however, helium ions are expected to be predominantly singly ionized with $He^+/He^{2+} > 1$ at $L \gtrsim 4$ and $E \lesssim 0.25$ MeV/nucleon (Spjeldvik and Fritz (1978a)). Thus it is conceivable that due to fast diffusive radial transport the high He^+/He^{2+}-ratios which most likely exist at large L-values in the lower energy range, will appear at low L-values in the high energy range. There, singly ionized helium can be observed for a few days before it decays by charge-exchange with neutral hydrogen of the earth's exosphere. The high He^+/He^{2+} observed at $L = 3.2$–3.6 could, therefore, be explained, at least qualitatively, by nonstationary processes in the magnetosphere. Whether this scenario provides a quantitative explanation for both the high He^+/He^{2+}-ratio at $L = 3.3$ and the sudden decrease above $L = 3.3$ can be verified only by solving the time dependent transport equations for He^+ and He^{2+}, including the simultaneous radial diffusive transport, the charge exchange processes and Coulomb energy loss as discussed above. However, such an analysis has not yet been performed.

In addition to time dependent effects, non-adiabatic processes, as the violation of the first adiabatic invariant, may play an important role. This has been suggested by Hovestadt et al. (1978a) in order to explain the absence of iron ($Fe/O < 0.01$) at energies of 0.4–1.5 MeV/nucleon in the trapping region of the outer radiation belt. A simple criterion, which can be used to separate adiabatic and non-adiabatic particle motion, is the Alfvén criterion which states that for adiabatic motion the gyroradius ρ of the particles has to be small compared with the scale length of the perpendicular magnetic field gradient:

$$\rho \cdot \left| \frac{\nabla B}{B} \right| \lesssim 0.1.$$

The gyroradii of iron and oxygen ions at the same energy/nucleon differ by only a factor of ~ 2. Therefore, if the interpretation of Hovestadt et al. (1978a) holds, small differences in rigidity result in large intensity differences of the trapped particle distribution. The gyroradii of He^+ and He^{2+} in the energy range of our measurements are comparable to the gyroradii of iron and oxygen in the energy range investigated by Hovestadt et al. (1978a). Rigidity dependent processes which suppress iron ions relative to oxygen and carbon in the outer radiation belt must therefore also influence the distribution of singly ionized helium relative to doubly ionized helium.

In summary, we found high abundances of singly ionized helium ($He^+/He^{2+} = 0.4 \pm 0.1$) at $L = 3.3$ during one perigee pass of ISEE-1 on 17 Nov 1977, with a sudden decrease of the He^+/He^{2+} ratio by a factor of ~ 10 between $L = 3.3$ and 3.7. We have shown that non-stationary and/or non-adiabatic processes may play an important role for the distribution of helium ions in the outer radiation belt. To clarify whether this is a persistent feature, a more systematic study of singly and doubly ionized helium during quiet and disturbed time periods is currently in progress.

Acknowledgements. The authors are grateful to the many individuals at the Max-Planck-Institut and the University of Maryland who have contributed to the success of the ISEE-mission. In particular, we thank J. Cain, H. Höfner, E. Künneth, P. Laeverenz, and E. Tums for designing and preparing the experiment for launch. We acknowledge helpful discussions with W.N. Spjeldvik. This work has been supported by NASA under contract NAS5-20062 and by the Bundesministerium für Forschung und Technologie, FRG, under contract number RC14-B8/74.

References

Allison, S.K.: Experimental results on charge-changing collisions of hydrogen and helium atoms and ions at kinetic energies above 0.2 keV, Rev. Mod. Phys. **30**, 1137–1168, 1958

Balsiger, H., Eberhardt, P., Geiss, J., Young, D.T.: Magnetic storm injection of 0.9 to 16 keV/e solar and terrestrial ions into the high-altitude magnetosphere. J. Geophys. Res. **85**, 1645–1662, 1980

Blake, J.B., Paulikas, G.A.: Geomagnetically trapped alpha particles, 1. Off-equator particles in the outer zone. J. Geophys. Res. **77**, 3431–3440, 1972

Blake, J.B.: Experimental test to determine the origin of geomagnetically trapped radiation. J. Geophys. Res. **78**, 5822–5824, 1973

Blake, J.B., Fennell, J.F., Hovestadt, D.: Measurements of heavy ions in the low-altitude regions of the outer zone. J. Geophys. Res. **85**, 5992–5996, 1980

Cornwall, J.M.: Radial diffusion of ionized helium and protons; a probe for magnetospheric dynamics. J. Geophys. Res. **77**, 1756–1770, 1972

Fälthammar, C.G.: Effects of time-dependent electric fields on geomagnetically trapped radiation. J. Geophys. Res. **70**, 2503–2516, 1965

Fennell, J.F., Blake, J.B., Paulikas, G.A.: Geomagnetically trapped alpha particles, 3. Low altitude outer zone alpha-proton comparisons. J. Geophys. Res. **79**, 521–528, 1974

Fritz, T.A., Williams, D.J.: Initial observations of geomagnetically trapped alpha-particles at the equator. J. Geophys. Res. **78**, 4719–4723, 1973

Fritz, T.A., Spjeldvik, W.N.: Observations of energetic radiation belt helium ions at the geomagnetic equator during quiet conditions. J. Geophys. Res. **83**, 2579–2583, 1978

Fritz, T.A., Spjeldvik, W.N.: Pitch angle distributions of geomagnetically trapped MeV helium ions during quiet times. J. Geophys. Res. **87**, 5095–5101, 1982

Holzworth, R.H., Mozer, F.S.: Direct evaluation of the radial diffusion coefficient near L = 6 due to electric field fluctuations. J. Geophys. Res. **84**, 2559–2566, 1979

Hovestadt, D., Gloeckler, G., Fan, C.Y., Fisk, L.A., Ipavich, F.M., Klecker, B., O'Gallagher, J.J., Scholer, M.: Evidence for solar

wind origin of energetic heavy ions in the earth's radiation belt. Geophys. Res. Lett. **5**, 1055–1057, 1978a

Hovestadt, D., Gloeckler, G., Fan, C.Y., Fisk, L.A., Ipavich, F.M., Klecker, B., O'Gallagher, J.J., Scholer, M., Arbinger, H., Cain, J., Höfner, H., Künneth, E., Laeverenz, P., Tums, E.: The nuclear and ionic charge distribution particle experiments on the ISEE-1 and ISEE-C spacecraft. IEEE, Transaction on Geoscience Electronics, **GE-16**, 166–175, 1978b

Hovestadt, D., Klecker, B., Mitchell, E., Fennell, J.E., Gloeckler, G., Fan, C.Y.: Spatial distribution of $Z \geqq 2$ ions in the outer radiation belt during quiet conditions. Adv. Space Res. **1**, 305–308, 1981a

Hovestadt, D., Gloeckler, G., Klecker, B., Ipavich, F.M., Fan, C.Y., Fisk, L.A., O'Gallagher, J.J., Scholer, M.: Singly charged energetic helium emitted in solar flares. Astrophys. J. **246**, L81–L84, 1981b

Krimigis, S.M.: The charge composition aspect of energetic trapped particles. In: Solar-Terrestrial Relations, p. 207. Calgary, Canada: University of Calgary 1973

Krimigis, S.M.: Alpha particles trapped in the earth's magnetic field. In: Particles and fields in the magnetosphere, B.M. McCormac, ed.: p. 364. Dordrecht, Holland: D. Reidel Publ. Co. 1970

Lyons, L.R., Evans, D.S.: The inconsistency between proton charge exchange and the observed ring current decay. J. Geophys. Res. **81**, 6197–6200, 1976

Lyons, L.R., Williams, D.J.: A source for the geomagnetic storm main phase ring current. J. Geophys. Res. **85**, 523–530, 1980

Mozer, F.S.: Power spectra of the magnetospheric electric field. J. Geophys. Res. **76**, 3651–3667, 1971

Pivovar, L.I., Tubaev, V.M., Novikov, M.T.: Electron loss and capture by 200–1500 keV helium ions in various gases. Soviet Physics JETP, **14**, 20–24, 1962

Sharp, R.D., Johnson, R.G., Shelley, E.G., Harris, K.K.: Energetic O^+ ions in the magnetosphere. J. Geophys. Res. **79**, 1844–1850, 1974

Sharp, R.D., Shelley, E.G., Johnson, R.G.: A search for helium ions in the recovery phase of a geomagnetic storm. J. Geophys. Res. **82**, 2361–2366, 1977

Shelley, E.G., Johnson, R.G., Sharp, R.D.: Satellite observations of energetic heavy ions during a geomagnetic storm. J. Geophys. Res. **77**, 6104–6110, 1972

Spjeldvik, W.N.: Equilibrium structure of equatorially mirroring radiation belt protons. J. Geophys. Res. **82**, 2801–2808, 1977

Spjeldvik, W.N., Fritz, T.A.: Energetic ionized helium in the quiet time radiation belts: Theory and comparison with observation. J. Geophys. Res. **83**, 654–662, 1978a

Spjeldvik, W.N., Fritz, T.A.: Theory for charge states of energetic oxygen ions in the earth's radiation belts. J. Geophys. Res. **83**, 1583–1594, 1978b

Spjeldvik, W.N., Fritz, T.A.: Observations of energetic helium ions in the earth's radiation belts during a sequence of geomagnetic storms. J. Geophys. Res. **86**, 2317–2328, 1981

Tinsley, B.A.: Evidence that the recovery phase ring current consists of helium ions. J. Geophys. Res. **81**, 6193–6196, 1976

Received December 3, 1982; Revised version February 2, 1983
Accepted February 17, 1983